

Large-scale lognormal fluctuations in turbulence velocity fields

Hideaki Mouri,^{1,a} Akihiro Hori,^{1,b} and Masanori Takaoka²

¹*Meteorological Research Institute, Nagamine, Tsukuba 305-0052, Japan*

²*Department of Mechanical Engineering, Doshisha University, Kyotanabe, Kyoto 610-0321, Japan*

(Dated: January 12, 2019)

For several flows of laboratory turbulence, we obtain long records of velocity data. These records are divided into segments. In each segment, we calculate the mean rate of energy dissipation, the mean energy at each scale, and the mean total energy. Their values fluctuate significantly among the segments. The fluctuations are lognormal, if the segment length lies within the range of large scales where the velocity correlations are insignificant but not yet absent. Since the lognormality is observed regardless of the Reynolds number and the configuration for turbulence production, it is expected to be universal. The likely origin is some multiplicative stochastic process related to interactions among many scales through the energy transfer.

I. INTRODUCTION

Turbulence spans a wide range of scales, from small scales in the dissipation and inertial subranges to large scales in the energy-containing subrange. While the small scales have been studied in detail,¹ the large scales have not thus far. There could remain some unknown features that are crucial to understand the fundamental physics of turbulence. Here, we reveal that the rate of energy dissipation, the energy at each scale, and the total energy fluctuate significantly over large scales in lognormal distributions. The lognormality is expected to be universal because it is observed regardless of the Reynolds number and the configuration for turbulence production.

Landau² was the first to discuss such a large-scale fluctuation. The discussion was that the local rate of energy dissipation ε should fluctuate significantly in space over large scales.

Obukhov³ also discussed the large-scale ε fluctuation. The ε fluctuation was assumed to be lognormal. This is because the fluctuation of any positive quantity could be approximated by a lognormal distribution with appropriate values for the average and standard deviation.

The large-scale fluctuations are known to exist on some level,^{4,5} but their details are not known. Experimentally or numerically, any detailed study requires long data that are composed of numerous ensembles. Each ensemble is required to cover smallest to largest scales of turbulence. Such long data have not been available. The situation is nevertheless improving for laboratory experiments, owing to improvements of the measurement technologies.

We have accordingly undertaken experimental studies of large-scale fluctuations.^{6,7} By using long velocity data obtained in a wind tunnel, we have shown that the large-scale fluctuations are always significant.⁶ Their standard deviations are comparable to the averages. Also for a case of grid turbulence, we have shown that the large-scale

fluctuations of the energy dissipation rate, the energy at each scale, and the total energy are lognormal.⁷

The next problem is whether the large-scale lognormal fluctuations exist in other turbulent flows. For grid turbulence, boundary layers, and jets at different Reynolds numbers, we show that the lognormal fluctuations do exist. The standard deviations are almost the same among the flows. It is thereby implied that the lognormality is not a mere approximation³ but is due to some common process. We discuss this and other implications.

II. EXPERIMENTS

Table I shows experimental conditions and turbulence parameters for grid turbulence (G1 and G2), boundary layers (B1 and B2), and jets (J1 and J2). The dataset G2 is from our previous work.⁷ We note that G2 and B1 as well as B2 and J1 have similar values of the microscale Reynolds number Re_λ .

A. Wind tunnel and anemometer

The experiments were carried out in a wind tunnel of the Meteorological Research Institute. We adopt coordinates x , y , and z in the streamwise, spanwise, and floor-normal directions. The corresponding flow velocities are $U + u$, v , and w . Here U is the average while u , v , and w are the fluctuations. The origin $x = y = z = 0$ m is on the center of the floor at the entrance to the test section of the wind tunnel. Its size was $\delta x = 18$ m, $\delta y = 3$ m, and $\delta z = 2$ m.

The wind tunnel had an air conditioner. If necessary, the conditioner was used to prevent the variation of air temperature. The resultant variation was ± 1 °C at most in each experiment, where the kinematic viscosity ν is assumed to have been constant.

To simultaneously measure $U + u$ and v , we used a hot-wire anemometer. The anemometer was composed of a constant temperature system and a crossed-wire probe. The wires were made of platinum-plated tungsten, 5 μ m

^aElectronic address: hmouri@mri-jma.go.jp

^bAlso at Meteorological and Environmental Sensing Technology, Inc., Nanpeidai, Ami 300-0312, Japan

TABLE I: Experimental conditions and turbulence parameters for grid turbulence (G1 and G2), boundary layers (B1 and B2), and jets (J1 and J2). The velocity derivative was obtained as $\partial_x v = [8v(x + \delta x) - 8v(x - \delta x) - v(x + 2\delta x) + v(x - 2\delta x)]/12\delta x$ with $\delta x = U/f_s$.

Quantity		Units	G1	G2	B1	B2	J1	J2
Measurement position	x	m	3.5	4.0	12.5	12.5	15.5	15.5
Measurement position	z	m	1.00	1.00	0.35	0.25	0.40	0.40
Mean streamwise velocity	U	m s^{-1}	12.75	21.16	3.118	11.34	11.48	17.38
Sampling frequency	f_s	kHz	40	70	10	60	44	70
Kinematic viscosity	ν	$\text{cm}^2 \text{s}^{-1}$	0.143	0.142	0.138	0.143	0.139	0.139
Mean energy dissipation rate	$\langle \varepsilon \rangle = 15\nu \langle (\partial_x v)^2 \rangle / 2$	$\text{m}^2 \text{s}^{-3}$	2.81	7.98	0.244	12.6	2.60	7.52
Kolmogorov velocity	$u_K = (\nu \langle \varepsilon \rangle)^{1/4}$	m s^{-1}	0.0796	0.103	0.0428	0.116	0.0776	0.101
Rms velocity fluctuation	$\langle u^2 \rangle^{1/2}$	m s^{-1}	0.696	1.10	0.552	2.37	1.56	2.34
Rms velocity fluctuation	$\langle v^2 \rangle^{1/2}$	m s^{-1}	0.683	1.06	0.464	1.96	1.36	2.06
Skewness factor	$\langle u^3 \rangle / \langle u^2 \rangle^{3/2}$		+0.08	+0.06	-0.22	-0.10	-0.04	-0.04
Skewness factor	$\langle v^3 \rangle / \langle v^2 \rangle^{3/2}$		-0.01	-0.01	+0.01	-0.01	+0.01	+0.01
Flatness factor	$\langle u^4 \rangle / \langle u^2 \rangle^2$		3.00	3.02	2.69	2.69	2.60	2.59
Flatness factor	$\langle v^4 \rangle / \langle v^2 \rangle^2$		2.98	3.00	3.06	3.05	3.05	3.06
Kolmogorov length	$\eta = (\nu^3 / \langle \varepsilon \rangle)^{1/4}$	cm	0.0180	0.0138	0.0322	0.0123	0.0179	0.0137
Taylor microscale	$\lambda = [2\langle v^2 \rangle / \langle (\partial_x v)^2 \rangle]^{1/2}$	cm	0.597	0.548	1.35	0.806	1.21	1.08
Correlation length	$L_u = \int_0^\infty \langle u(x+r)u(x) \rangle dr / \langle u^2 \rangle$	cm	17.5	17.9	49.0	43.0	128.	124.
Correlation length	$L_v = \int_0^\infty \langle v(x+r)v(x) \rangle dr / \langle v^2 \rangle$	cm	4.46	4.69	6.94	5.68	10.2	10.2
Microscale Reynolds number	$\text{Re}_\lambda = \langle v^2 \rangle^{1/2} \lambda / \nu$		285	409	454	1103	1183	1603

in diameter, 1.25 mm in sensing length, 1 mm in separation, oriented at $\pm 45^\circ$ to the streamwise direction, and 280 °C in temperature.

space randomly and independently.^{8,9} Not always close to the Gaussian values are $\langle u^3 \rangle / \langle u^2 \rangle^{3/2}$ and $\langle u^4 \rangle / \langle u^2 \rangle^2$. They tend to be sensitive to largest scale motions induced by either the grid, roughness, or nozzle.

B. Flow configurations

For the grid turbulence, we placed a grid at $x = 0$ m across the entrance to the test section of the wind tunnel. The grid was composed of two layers of uniformly spaced rods, with axes in the two layers at right angles. The cross section of the rod was $0.04 \times 0.04 \text{ m}^2$. The spacing of the axes of adjacent rods was 0.20 m. We set the incoming flow velocity to be 12 m s^{-1} (G1) or 20 m s^{-1} (G2). The measurement position was on the tunnel axis.

For the boundary layers, roughness blocks were placed over the entire floor of the test section. The block size was $\delta x = 0.06$ m, $\delta y = 0.21$ m, and $\delta z = 0.11$ m. The spacing of the centers of adjacent blocks was $\delta x = \delta y = 0.50$ m. We set the incoming flow velocity to be 4 m s^{-1} (B1) or 16 m s^{-1} (B2). The measurement position was in the log-law sublayer at $x = 12.5$ m and $y = 0$ m, where the boundary layer had the displacement thickness of 0.2 m and the 99% velocity thickness of 0.8 m.

For the jets, we placed a contraction nozzle. Its exit was at $x = -2$ m and was rectangular with the size $\delta y = 2.1$ m and $\delta z = 1.4$ m. The center was on the tunnel axis. We set the flow velocity at the nozzle exit to be 16 m s^{-1} (J1) or 24 m s^{-1} (J2). The measurement position was at $x = 15.5$ m, $y = 0$ m, and $z = 0.40$ m. Although the position might appear to have been too close to the floor of the test section, this does not matter to our study.

The skewness factor $\langle v^3 \rangle / \langle v^2 \rangle^{3/2}$ and the flatness factor $\langle v^4 \rangle / \langle v^2 \rangle^2$ at the measurement position were always close to the Gaussian values of 0 and 3. Here $\langle \cdot \rangle$ denotes an average. These Gaussian values imply that turbulence had been well developed and various eddies filled the

C. Data sampling and processing

The anemometer signal was linearized, low-pass filtered, and then digitally sampled. We set the sampling frequency as high as possible, on the condition that high-frequency noise was not seen in the power spectrum. The filter cutoff was at one-half of the sampling frequency. We obtained a long record of 4×10^8 data in each experiment, except for 1×10^8 data in B1.

The anemometer signal is proportional to the flow velocity, through the calibration coefficient that depends on the condition of the anemometer and thereby varied slowly in time. For individual segments of the data records, the length of which is fixed for each record and ranges from 4×10^6 to 2×10^7 data, we determined the coefficient so as to have the same U value. The coefficient within each segment is estimated to have varied by $\pm 1\%$ at most.

We converted $u(t)$ and $v(t)$ at time t into $u(x)$ and $v(x)$ at position x , by using Taylor's frozen-eddy hypothesis, $x = -Ut$, which requires that $\langle u^2 \rangle^{1/2} / U$ is small enough. This requirement was satisfied in our experiments where $\langle u^2 \rangle^{1/2} / U \lesssim 0.2$. Even at $\langle u^2 \rangle^{1/2} / U \simeq 0.3$, Taylor's hypothesis holds valid as demonstrated by data obtained simultaneously with two probes separated by streamwise distances.¹⁰

Since $u(t)$ and $v(t)$ are stationary, $u(x)$ and $v(x)$ are homogeneous, although actual turbulence in the wind tunnel was not homogeneous along the x direction. Over small scales, fluctuations of $u(x)$ and $v(x)$ correspond to spatial fluctuations that actually existed in the wind tun-

TABLE II: Statistics of $\ln \delta u_{r,R}^2$ and $\ln \delta v_{r,R}^2$ at $r/L_u = 0.01, 0.03$, and 0.1 as well as of $\ln \delta u_R^2$ and $\ln \delta v_R^2$ among segments with $R/L_u = 10$ for grid turbulence (G1 and G2), boundary layers (B1 and B2), and jets (J1 and J2). We also show the number of the segments used for the analyses.

Quantity	G1	G2	B1	B2	J1	J2
Standard deviation						
$\ln \delta u_{0.01L_u,R}^2$	0.15	0.14	0.17	0.15	0.11	0.11
$\ln \delta u_{0.03L_u,R}^2$	0.14	0.14	0.16	0.16	0.12	0.12
$\ln \delta u_{0.1L_u,R}^2$	0.16	0.16	0.18	0.18	0.14	0.14
$\ln u_R^2$	0.31	0.32	0.35	0.35	0.25	0.26
$\ln \delta v_{0.01L_u,R}^2$	0.15	0.14	0.16	0.14	0.12	0.12
$\ln \delta v_{0.03L_u,R}^2$	0.14	0.14	0.15	0.15	0.13	0.13
$\ln \delta v_{0.1L_u,R}^2$	0.16	0.16	0.17	0.17	0.15	0.15
$\ln v_R^2$	0.22	0.23	0.25	0.25	0.20	0.20
Skewness factor						
$\ln \delta u_{0.01L_u,R}^2$	-0.00	+0.06	-0.03	+0.02	-0.03	-0.06
$\ln \delta u_{0.03L_u,R}^2$	+0.00	+0.06	-0.02	+0.04	-0.05	-0.02
$\ln \delta u_{0.1L_u,R}^2$	-0.02	+0.05	-0.00	-0.01	-0.02	-0.04
$\ln u_R^2$	+0.19	+0.22	+0.19	+0.08	-0.02	-0.00
$\ln \delta v_{0.01L_u,R}^2$	-0.01	+0.04	-0.13	-0.07	-0.03	-0.05
$\ln \delta v_{0.03L_u,R}^2$	+0.01	+0.05	-0.07	-0.05	-0.04	-0.05
$\ln \delta v_{0.1L_u,R}^2$	+0.00	+0.03	-0.07	-0.07	-0.02	-0.07
$\ln v_R^2$	+0.03	+0.05	+0.01	+0.01	-0.06	-0.01
Flatness factor						
$\ln \delta u_{0.01L_u,R}^2$	2.94	3.00	3.02	3.13	3.02	3.07
$\ln \delta u_{0.03L_u,R}^2$	2.95	3.01	3.00	3.09	3.06	3.06
$\ln \delta u_{0.1L_u,R}^2$	2.97	3.01	3.02	3.09	3.02	2.98
$\ln u_R^2$	3.02	3.03	3.21	2.95	3.11	2.95
$\ln \delta v_{0.01L_u,R}^2$	2.95	3.00	3.11	3.14	3.04	2.98
$\ln \delta v_{0.03L_u,R}^2$	2.97	3.01	3.07	3.10	3.00	3.05
$\ln \delta v_{0.1L_u,R}^2$	2.99	3.01	3.03	3.01	2.97	3.03
$\ln v_R^2$	3.00	3.03	2.95	2.97	2.93	2.91
Correlation coefficient against $\ln v_R^2$						
$\ln \delta u_{0.01L_u,R}^2$	+0.34	+0.35	+0.37	+0.37	+0.36	+0.36
$\ln \delta u_{0.03L_u,R}^2$	+0.32	+0.33	+0.37	+0.35	+0.36	+0.36
$\ln \delta u_{0.1L_u,R}^2$	+0.28	+0.29	+0.36	+0.32	+0.31	+0.33
$\ln u_R^2$	+0.10	+0.12	-0.02	-0.05	-0.04	-0.03
$\ln \delta v_{0.01L_u,R}^2$	+0.36	+0.37	+0.27	+0.30	+0.32	+0.33
$\ln \delta v_{0.03L_u,R}^2$	+0.39	+0.39	+0.31	+0.33	+0.36	+0.36
$\ln \delta v_{0.1L_u,R}^2$	+0.49	+0.49	+0.41	+0.41	+0.50	+0.49
Number of segments						
N_R	72600	67600	12730	17560	8120	8000

nel. Those over large scales do not. They are interpreted as fluctuations over long timescales described in terms of large length scales.¹¹

To calculate small-scale statistics such as the mean rate of energy dissipation $\langle \varepsilon \rangle$, we used $\partial_x v$ instead of usual $\partial_x u$ by assuming local isotropy $\langle (\partial_x v)^2 \rangle = 2 \langle (\partial_x u)^2 \rangle$. Over smallest scales, the u component measured by a crossed-wire probe is contaminated with the w component that is perpendicular to the two wires of the probe.¹² The v component is free from such contamination.

III. RESULTS AND DISCUSSION

The data records are divided into segments with length R . For each segment, the center of which is defined as

x_c , we calculate the mean energies at scale $r < R$ as

$$\delta u_{r,R}^2(x_c) = \frac{1}{R-r} \int_{x_c-R/2}^{x_c+R/2-r} \delta u_r^2(x) dx, \quad (1a)$$

$$\delta v_{r,R}^2(x_c) = \frac{1}{R-r} \int_{x_c-R/2}^{x_c+R/2-r} \delta v_r^2(x) dx, \quad (1b)$$

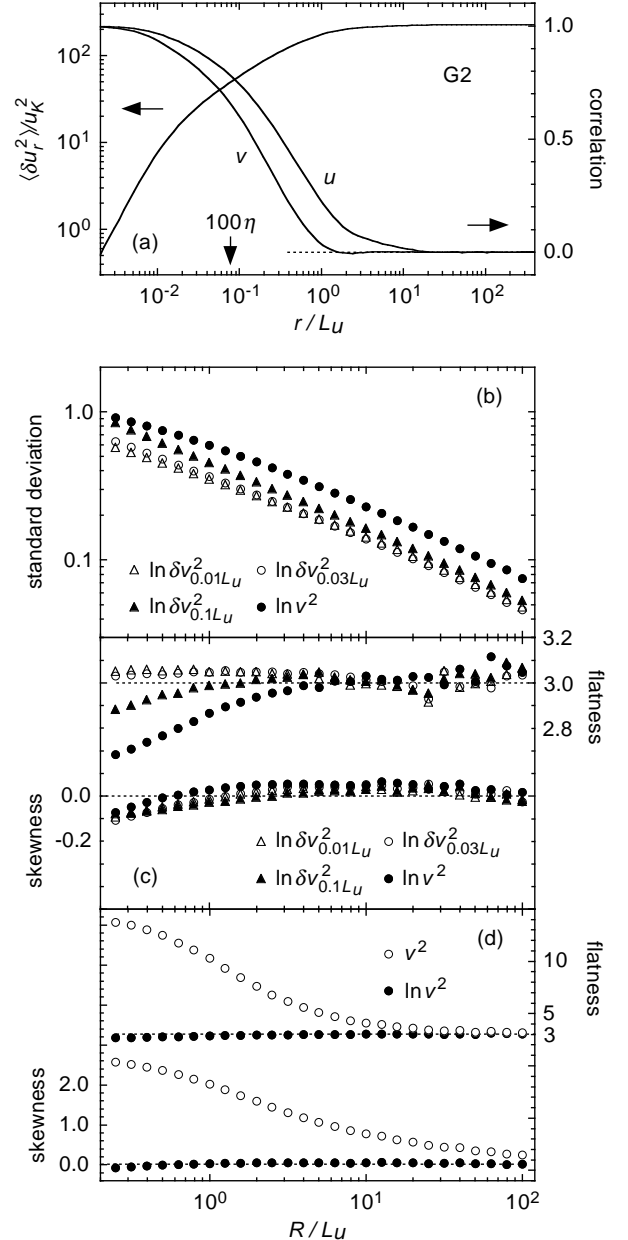


FIG. 1: Statistics for grid turbulence G2 as a function of r/L_u or R/L_u . (a) $\langle u(x+r)u(x) \rangle / \langle u^2 \rangle$, $\langle v(x+r)v(x) \rangle / \langle v^2 \rangle$, and $\langle \delta u_r^2 \rangle / u_K^2$. The arrow indicates the scale $r = 100\eta$. (b) Standard deviations of $\ln \delta v_{0.01L_u,R}^2$ (Δ), $\ln \delta v_{0.03L_u,R}^2$ (\circ), $\ln \delta v_{0.1L_u,R}^2$ (\blacktriangle), and $\ln v_R^2$ (\bullet). (c) Skewness and flatness factors of $\ln \delta v_{0.01L_u,R}^2$ (Δ), $\ln \delta v_{0.03L_u,R}^2$ (\circ), $\ln \delta v_{0.1L_u,R}^2$ (\blacktriangle), and $\ln v_R^2$ (\bullet). (d) Skewness and flatness factors of v_R^2 (\circ) and $\ln v_R^2$ (\bullet).

with $\delta u_r(x) = u(x+r) - u(x)$ and $\delta v_r(x) = v(x+r) - v(x)$. The mean total energies are also calculated as

$$u_R^2(x_c) = \frac{1}{R} \int_{x_c-R/2}^{x_c+R/2} u^2(x) dx, \quad (2a)$$

$$v_R^2(x_c) = \frac{1}{R} \int_{x_c-R/2}^{x_c+R/2} v^2(x) dx. \quad (2b)$$

Statistics of these coarse-grained quantities are studied as a function of R . The results are summarized in Figs. 1–3 and Table II.

The segment length R is given in units of the correlation length L_u . This is the representative of large scales.

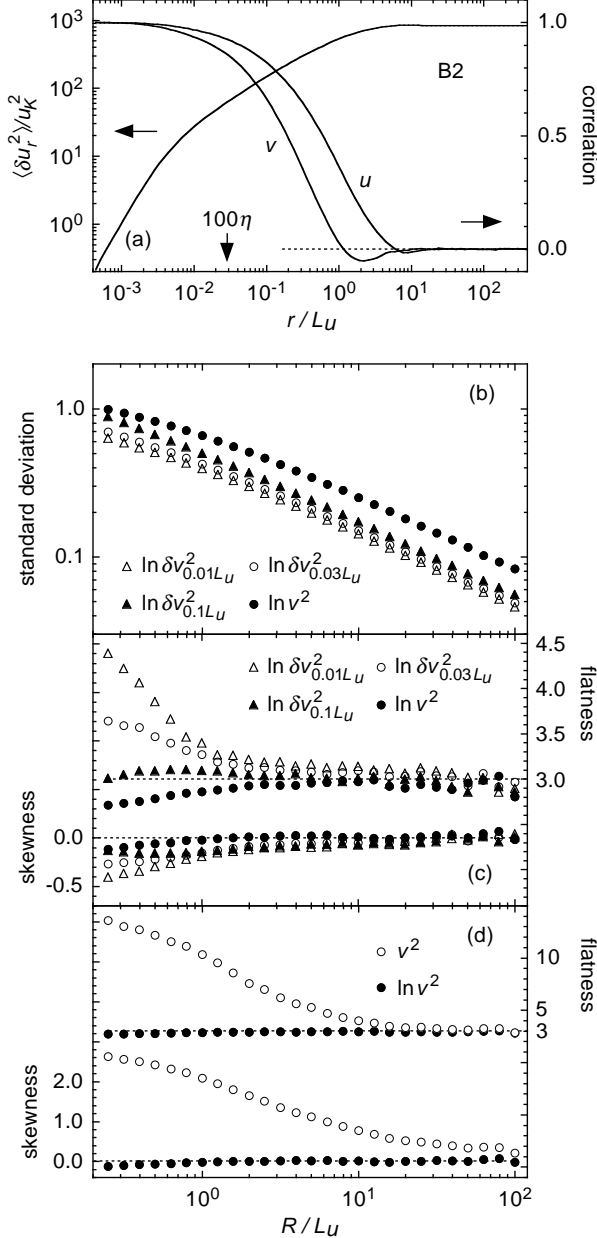


FIG. 2: Same as in Fig. 1 but for boundary layer B2.

Up to about $10^0 L_u$, the correlations $\langle u(x+R)u(x) \rangle$ and $\langle v(x+R)v(x) \rangle$ are significant [Figs. 1(a), 2(a), and 3(a)]. They are insignificant but not yet absent at about $10^0 L_u - 10^2 L_u$, which is the R range of our main interest. The scale r is also given in units of L_u as $0.01L_u$, $0.03L_u$ or $0.1L_u$. At $r/L_u \rightarrow \infty$, $\delta u_{r,R}^2$ and $\delta v_{r,R}^2$ correspond to u_R^2 and v_R^2 in a statistical sense.

A. Significance of large-scale fluctuations

Figures 1(b), 2(b), and 3(b) show the standard deviations of $\ln \delta v_{r,R}^2$ and $\ln v_R^2$ as a function of R/L_u . For

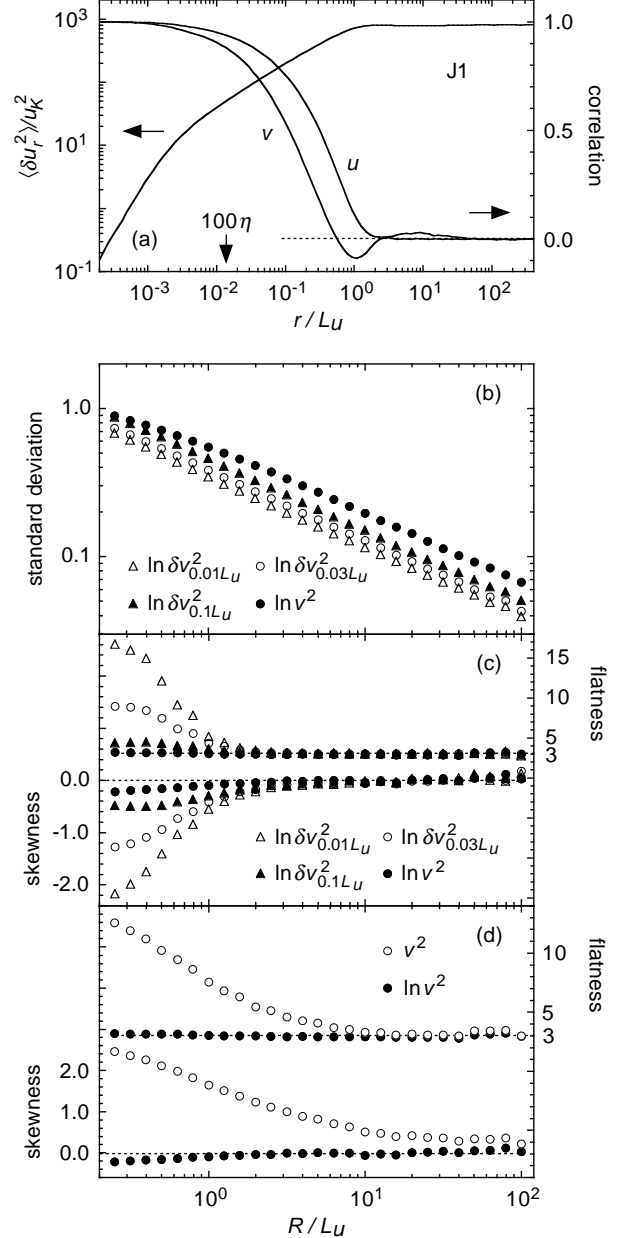


FIG. 3: Same as in Fig. 1 but for turbulent jet J1.

example, the standard deviation of $\ln v_R^2$ is

$$\langle (\ln v_R^2 - \langle \ln v_R^2 \rangle)^2 \rangle^{1/2}. \quad (3)$$

The average is over all the segments. With an increase of R , the standard deviations decrease, but they are not so small even at largest R . Thus, large-scale fluctuations of δv_r^2 and v^2 are significant.^{6,7} The same is true for δu_r^2 and u^2 (Table II).

If we fix R/L_u and r/L_u , the standard deviations of $\ln \delta u_{r,R}^2$, $\ln \delta v_{r,R}^2$, and $\ln v_R^2$ are almost the same among the datasets. This implies the existence of some common process. The exception is $\ln u_R^2$ that suffers from largest scale motions of the flow (Sec. II B). With an increase of r , the standard deviations of $\ln \delta u_{r,R}^2$ and $\ln \delta v_{r,R}^2$ tend to increase.

B. Lognormality of large-scale fluctuations

Figures 1(c), 2(c), and 3(c) show the skewness and flatness factors of $\ln \delta v_{r,R}^2$ and $\ln v_R^2$. For example, the skewness factor of $\ln v_R^2$ is

$$\frac{\langle (\ln v_R^2 - \langle \ln v_R^2 \rangle)^3 \rangle}{\langle (\ln v_R^2 - \langle \ln v_R^2 \rangle)^2 \rangle^{3/2}}. \quad (4a)$$

The flatness factor of $\ln v_R^2$ is

$$\frac{\langle (\ln v_R^2 - \langle \ln v_R^2 \rangle)^4 \rangle}{\langle (\ln v_R^2 - \langle \ln v_R^2 \rangle)^2 \rangle^2}. \quad (4b)$$

At $R/L_u \simeq 10^0$ – 10^2 , the skewness and flatness factors are close to the Gaussian values of 0 and 3. Thus, large-scale fluctuations of δv_r^2 and v^2 are lognormal. The lognormality is expected to be universal because it is observed in all the datasets. They are different in the Reynolds number or the flow configuration. Also for $\delta u_{r,R}^2$ (Table II), we observe the lognormality.

Figure 4 shows the probability density distributions of $\ln \delta v_{r,R}^2$ and $\ln v_R^2$ at $R/L_u = 10$. The distributions are Gaussian, at least in the observed range that extends to several standard deviations from the peak.

In some datasets, deviation from the lognormality is seen for u_R^2 (Table II). It tends toward the lognormality but suffers from largest scale motions of the flow (Sec. II B).

The lognormal fluctuations observed here are distinct from those modelled by Kolmogorov.¹³ While he was interested in small-scale intermittency¹ and studied δu_r^n at small r to obtain their scaling laws, we are interested in large-scale fluctuations and study $\delta u_{r,R}^n$ at large R . The scaling laws of $\delta u_{r,R}^n$ are not necessary. Thus, our study is not necessarily concerned with the well-known problems of Kolmogorov's lognormal model, e.g., violation of Novikov's inequality¹⁴ for scaling exponents. In addition, we are not intended to argue that the lognormality is exact (Sec. III E).

C. Correlation among large-scale fluctuations

Table II shows the correlation coefficients of $\ln \delta u_{r,R}^2$, $\ln \delta v_{r,R}^2$, and $\ln u_R^2$ against $\ln v_R^2$. For example, the coefficient of $\ln \delta v_{r,R}^2$ is

$$\frac{\langle \ln \delta v_{r,R}^2 \ln v_R^2 \rangle - \langle \ln \delta v_{r,R}^2 \rangle \langle \ln v_R^2 \rangle}{\langle (\ln \delta v_{r,R}^2 - \langle \ln \delta v_{r,R}^2 \rangle)^2 \rangle^{1/2} \langle (\ln v_R^2 - \langle \ln v_R^2 \rangle)^2 \rangle^{1/2}}. \quad (5)$$

The correlations are significant for most of the quantities. They tend to fluctuate synchronously.

The datasets share interesting features. Between $\ln u_R^2$ and $\ln v_R^2$, the correlation is absent. With a decrease of

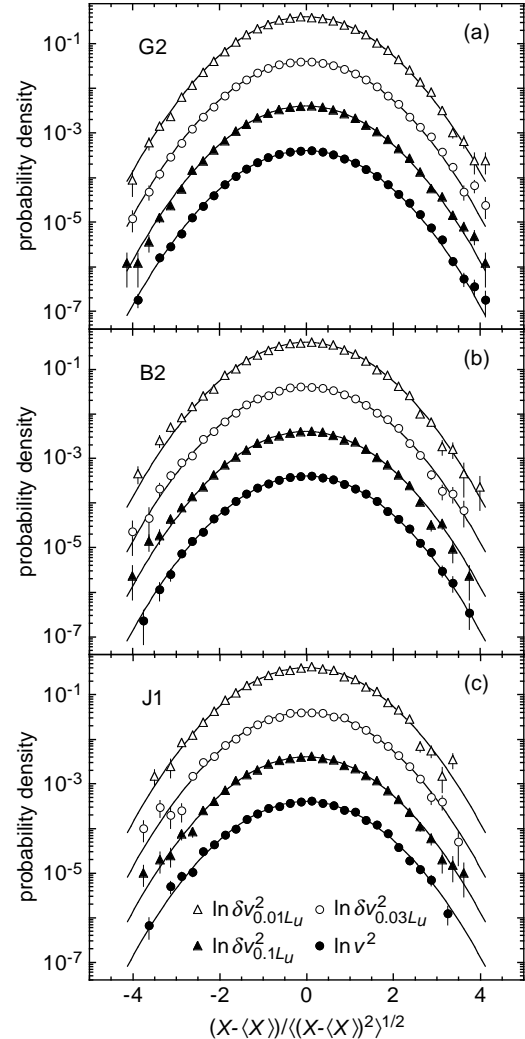


FIG. 4: Probability densities $P(X_R)$ of $X_R = \ln \delta v_{0.01L_u,R}^2$ (Δ), $\ln \delta v_{0.03L_u,R}^2$ (\circ), $\ln \delta v_{0.1L_u,R}^2$ (\blacktriangle), and $\ln v_R^2$ (\bullet) at $R/L_u = 10$ as a function of $(X_R - \langle X_R \rangle)/(\langle (X_R - \langle X_R \rangle)^2 \rangle)^{1/2}$. The error bars represent $P(X_R)/N_{X_R}^{1/2}$, where N_{X_R} is the number of segments that fall in the bin. The curves represent Gaussian distributions. They are individually shifted by a factor 10. (a) Grid turbulence G2. (b) Boundary layer B2. (c) Turbulent jet J1.

TABLE III: Same as in Table II but for $\ln \delta u_{r,R}^2$ and $\ln \delta v_{r,R}^2$ at $r/\eta = 30, 100$, and 300 as well as for $\ln \varepsilon_R$.

Quantity	G1	G2	B1	B2	J1	J2
Standard deviation						
$\ln \delta u_{30\eta,R}^2$	0.14	0.14	0.16	0.16	0.12	0.11
$\ln \delta u_{100\eta,R}^2$	0.16	0.15	0.17	0.16	0.12	0.12
$\ln \delta u_{300\eta,R}^2$	0.20	0.19	0.19	0.17	0.13	0.13
$\ln \varepsilon_R$	0.16	0.16	0.20	0.19	0.14	0.13
$\ln \delta v_{30\eta,R}^2$	0.14	0.14	0.15	0.14	0.11	0.11
$\ln \delta v_{100\eta,R}^2$	0.16	0.16	0.16	0.15	0.12	0.12
$\ln \delta v_{300\eta,R}^2$	0.20	0.19	0.19	0.17	0.13	0.13
Skewness factor						
$\ln \delta u_{30\eta,R}^2$	+0.00	+0.06	-0.02	+0.00	-0.03	-0.07
$\ln \delta u_{100\eta,R}^2$	-0.02	+0.06	-0.01	+0.04	-0.03	-0.05
$\ln \delta u_{300\eta,R}^2$	-0.02	+0.01	-0.01	+0.00	-0.04	-0.01
$\ln \varepsilon_R$	-0.00	+0.05	-0.15	-0.23	-0.04	-0.10
$\ln \delta v_{30\eta,R}^2$	+0.01	+0.05	-0.09	-0.09	-0.04	-0.08
$\ln \delta v_{100\eta,R}^2$	-0.00	+0.04	-0.06	-0.05	-0.03	-0.05
$\ln \delta v_{300\eta,R}^2$	-0.02	+0.01	-0.05	-0.07	-0.03	-0.06
Flatness factor						
$\ln \delta u_{30\eta,R}^2$	2.95	3.00	3.03	3.13	3.00	3.05
$\ln \delta u_{100\eta,R}^2$	2.97	3.01	3.04	3.09	3.02	3.06
$\ln \delta u_{300\eta,R}^2$	2.98	2.99	3.01	3.07	3.05	3.05
$\ln \varepsilon_R$	2.94	2.98	3.17	3.35	3.04	2.99
$\ln \delta v_{30\eta,R}^2$	2.97	3.01	3.06	3.15	3.02	2.97
$\ln \delta v_{100\eta,R}^2$	2.99	3.01	3.03	3.10	3.04	2.99
$\ln \delta v_{300\eta,R}^2$	2.97	3.01	3.06	3.01	2.97	3.05
Correlation coefficient against $\ln v_R^2$						
$\ln \delta u_{30\eta,R}^2$	+0.31	+0.33	+0.37	+0.37	+0.36	+0.36
$\ln \delta u_{100\eta,R}^2$	+0.28	+0.30	+0.36	+0.35	+0.36	+0.36
$\ln \delta u_{300\eta,R}^2$	+0.23	+0.25	+0.32	+0.33	+0.35	+0.35
$\ln \varepsilon_R$	+0.35	+0.36	+0.23	+0.25	+0.29	+0.29
$\ln \delta v_{30\eta,R}^2$	+0.39	+0.38	+0.29	+0.30	+0.32	+0.32
$\ln \delta v_{100\eta,R}^2$	+0.49	+0.46	+0.36	+0.33	+0.33	+0.33
$\ln \delta v_{300\eta,R}^2$	+0.65	+0.60	+0.52	+0.40	+0.38	+0.37
Number of segments						
N_R	72600	67600	12730	17560	8120	8000

r , the correlation of $\ln \delta u_{r,R}^2$ against $\ln v_R^2$ is increasingly significant, while that of $\ln \delta v_{r,R}^2$ is increasingly insignificant. Taking also account of the observed decrease of the standard deviations with a decrease of r (Sec. III A), we consider that the fluctuations originate in large r . Those in the u and v components are originally uncorrelated but become correlated in the course of their propagation to the smaller r .

D. Large-scale fluctuations of small-scale quantities

We studied $\delta u_{r,R}^2$ and $\delta v_{r,R}^2$ at $r/L_u = 0.01, 0.03$, and 0.1 . They are studied instead at $r/\eta = 30, 100$, and 300 . Here, the Kolmogorov length η is the representative of small scales. Judging from $\langle \delta u_r^2 \rangle$ in Figs. 1(a), 2(a), and 3(a), the scale 30η lies in the dissipation subrange. The scale 100η lies in the inertial subrange with $\langle \delta u_r^2 \rangle \propto r^{2/3}$. This subrange extends beyond 300η if the Reynolds number is high enough. We also study the energy dissipation rate averaged over each segment

$$\varepsilon_R(x_c) = \frac{1}{R} \int_{x_c - R/2}^{x_c + R/2} \varepsilon(x) dx, \quad (6)$$

with $\varepsilon = 15\nu(\partial_x v)^2/2$.¹⁵ It corresponds to δv_r^2 at $r/\eta \rightarrow 0$.

Table III shows the results at $R/L_u = 10$. The fluctuations are lognormal. The correlations against $\ln v_R^2$ have the same features as in Table II. However, with respect to the standard deviations at fixed r/L_u in Table II, those at fixed r/η in Table III tend to scatter among the datasets. Therefore, the fluctuations are described in terms of the correlation length L_u that represents large scales, rather than of the Kolmogorov length η that represents small scales (see also Sec. III C).

The standard deviation of $\ln \varepsilon_R$ is larger than that of $\ln \delta v_{30\eta,R}^2$, although the standard deviation of $\ln \delta v_{r,R}^2$ decreases with a decrease of r down to 30η . Probably, $\ln \varepsilon_R$ suffers from small-scale intermittency that causes a broad ε distribution.¹

For ε_R in the dataset B1 and B2, deviation from the lognormality is seen. The lognormality is achieved at the larger R . In fact, at $R/L_u = 100$, the skewness factor is +0.03 (B1) or +0.00 (B2), while the flatness factor is 3.04 (B1) or 3.00 (B2).

E. Origin of large-scale lognormal fluctuations

Regardless of the Reynolds number and the flow configuration, the energies δu_r^2 and δv_r^2 at scale r , the total energies u^2 and v^2 , and also the energy dissipation rate ε fluctuate over large scales in lognormal distributions (Sec. III B). Their standard deviations are almost the same among the flows (Sec. III A). Hence, some common process is at work, which is discussed here.

The observed fluctuations originate in turbulence itself. They are too strong to be an experimental artifact, i.e., some variation in the condition of the wind tunnel or the measurement system. In addition, if such a variation were responsible for the fluctuations, they should exhibit a correlation between u_R^2 and v_R^2 that is actually absent (Sec. III C).

A lognormal fluctuation is induced by some multiplicative stochastic process, e.g., a product of many independent stochastic variables, $Q_N = \prod_{n=1}^N q_n$. Its logarithm is a sum of many independent stochastic variables, $\ln Q_N = \sum_{n=1}^N \ln q_n$, which is Gaussian according to the central limit theorem. For the lognormal fluctuations observed here, the process is related to interactions among scales through the energy transfer.⁷ While the mean energy transfer is to a smaller scale and is significant between scales in the inertial subrange alone, the local energy transfer is either to a smaller or larger scale and is significant between all scales.^{6,16,17,18} Thus, any scale interacts with itself and with many other scales.

The fluctuations observed for different scales r tend to be synchronous (Sec. III C). This is consistent with the above explanation that the fluctuations are induced by interactions among scales.

The rate of the energy transfer does not have a lognormal fluctuation because the rate could change its sign.

Although the fluctuation of this rate is important, it is beyond the reach of our experimental study.

To apply the central limit theorem, there exist various forms of sufficient but not necessary conditions.¹⁹ The essence is that the stochastic variables are all alike and no few of them dominate the others. It is also required that, among the variables, correlations are absent exactly or at least practically. These requirements have to be satisfied by the interactions among scales that are to reproduce the observed lognormality.

The interactions are also required to involve a wide range of scales because the lognormal fluctuations are observed up to large R and down to small r . Large scales are especially important as implied by the observed features of the standard deviations and correlations (Secs. III A and III C).

The central limit theorem does not determine the distribution at its tail, which might deviate from the lognormal distribution and even might depend on the Reynolds number or the flow configuration. Whether such a tail is prominent depends on the case. An extreme case could be the observed deviation from the lognormality for u_R^2 in some datasets (Sec. III B). Nevertheless, the lognormality is important at least as an idealized model because it exists only if the logarithm is subject to the central limit theorem. The lognormality also accounts for most of the distributions in the observed range (Fig. 4). To observe the distributions over the wider range, much longer data are necessary.

F. Scale range of lognormal fluctuations

The lognormal fluctuations exist at $R/L_u \simeq 10^0\text{--}10^2$, where the correlations $\langle u(x+R)u(x) \rangle$ and $\langle v(x+R)v(x) \rangle$ are insignificant but not yet absent [Figs. 1(a), 2(a), and 3(a)]. Although their profiles are different there among the flow configurations, this difference is not relevant to the existence of the lognormality. Outside that R range, the correlations are either significant or absent. The lognormal fluctuations do not exist.

At $R/L_u \lesssim 10^0$, the skewness and flatness factors of $\ln \delta v_{r,R}^2$ and $\ln v_R^2$ deviate from the Gaussian values [Figs. 1(c), 2(c), and 3(c)]. The fluctuations are not lognormal and no longer explained by a multiple of independent processes. This is because the correlations $\langle u(x+R)u(x) \rangle$ and $\langle v(x+R)v(x) \rangle$ are too strong. The observed deviation from the lognormality is different among the dataset. Note that, among the figures, different are the ordinates for the skewness and flatness factors. Since this R range for small scales has been studied in detail,¹ we do not study it any more.

At $R/L_u \gtrsim 10^2$, the correlations $\langle u(x+R)u(x) \rangle$ and $\langle v(x+R)v(x) \rangle$ are absent. Then, any segment with length R is divisible into subsegments that are independent of one another. The length R_* of these subsegments is such that $L_u \ll R_* \ll R$. By using a sum over the subseg-

ments, we write ε_R , $\delta u_{r,R}^2$, $\delta v_{r,R}^2$, u_R^2 , and v_R^2 as, e.g.,

$$v_R^2(x_c) = \frac{R_*}{R} \sum_{n=1}^{R/R_*} v_{R_*}^2(x_{c_n}). \quad (7)$$

Here x_{c_n} is the center of the n -th subsegment. The sum is subject to the central limit theorem and thereby fluctuates in a Gaussian distribution.^{6,20} Figures 1(d), 2(d), and 3(d) show the skewness and flatness factors of v_R^2 , which in fact approach to the Gaussian values with an increase of R/L_u .²¹ In other words, when R/L_u is large enough, quantities such as Rv_R^2 are additive.⁶ The value of an additive quantity for a region is the sum of its values for the subregions that are independent of one another. Such additive quantities are well known in thermodynamics and statistical mechanics,²² for which correlations are absent over scales of interest.

IV. CONCLUDING REMARKS

For several flows of laboratory turbulence, we obtained long records of velocity data. These records were divided into segments with length R . In each segment, we calculated the mean rate of energy dissipation ε_R , the mean energies $\delta u_{r,R}^2$ and $\delta v_{r,R}^2$ at scale r , and the mean total energies u_R^2 and v_R^2 . Their values fluctuate significantly and synchronously. The fluctuations are lognormal. Since the lognormality is observed regardless of the Reynolds number and the configuration for turbulence production, it is expected to be universal.

The lognormal fluctuations are of large scales, $R/L_u \simeq 10^0\text{--}10^2$, where the correlations $\langle u(x+R)u(x) \rangle$ and $\langle v(x+R)v(x) \rangle$ are insignificant but not yet absent. This R range had not been studied, although it lies in between the ranges that had been studied in detail.

We explained the lognormal fluctuations by applying the central limit theorem to the logarithm of a multiplicative stochastic process, which was related to interactions among many scales through the energy transfer. To apply the central limit theorem, it is required that the interactions are all alike and do not have mutual correlations. In addition, features of the observed fluctuations require that the interactions involve a wide range of scales. Large scales are especially important.

The first discussion on large-scale fluctuations was by Landau,² who argued against the universality of small-scale statistics discussed by Kolmogorov.²³ Kolmogorov discussed that small-scale statistics depend on ν and $\langle \varepsilon \rangle$ alone and are thus universal. Landau discussed that small-scale statistics are not universal because the large-scale ε fluctuation is significant and is not universal. In practice, large-scale fluctuations are universally lognormal. Their standard deviations are also almost universal. Even if large scales affect small scales through the ε fluctuation,^{3,24} it does not necessarily violate the universality of small-scale statistics. However, past experi-

ments suggested that some small-scale statistics are not universal and depend on the large-scale flow.^{6,10,25,26,27} Since the Reynolds numbers of these studies might not have been high enough to distinguish between small and large scales,^{28,29} it is desirable to study the effect of large scales on small scales at the higher Reynolds numbers.

Finally, we note that the large-scale lognormal fluctuations are not limited to those of turbulence. They should also exist in other nonlinear systems that have many degrees of freedom. This is because, regardless of the process details, the lognormality exists only if the logarithm is subject to the central limit theorem. However, so far as we could see, no example is known. Hence, it is desirable

to explore the lognormal fluctuations in various systems, promisingly over length scales or timescales where correlations are insignificant but not yet absent. We expect that the large-scale lognormal fluctuations turn out to be ubiquitous, far beyond those of turbulence observed here.

Acknowledgments

The authors are grateful to Y. Kawashima for his help in our experiments.

¹ K. R. Sreenivasan and R. A. Antonia, “The phenomenology of small-scale turbulence,” *Annu. Rev. Fluid Mech.* **29**, 435 (1997).

² L. D. Landau and E. M. Lifshitz, *Fluid Mechanics* (Pergamon, London, 1959), Chap. 3. Landau formulated his discussion in the temporal domain. We recast it in the spatial domain.

³ A. M. Obukhov, “Some specific features of atmospheric turbulence,” *J. Fluid Mech.* **13**, 77 (1962).

⁴ A. Praskovsky and S. Oncley, “Comprehensive measurements of the intermittency exponent in high Reynolds number turbulent flows,” *Fluid Dyn. Res.* **21**, 331 (1997).

⁵ J. Cleve, M. Greiner, and K. R. Sreenivasan, “On the effects of surrogacy of energy dissipation in determining the intermittency exponent in fully developed turbulence,” *Europhys. Lett.* **61**, 756 (2003).

⁶ H. Mouri, M. Takaoka, A. Hori, and Y. Kawashima, “On Landau’s prediction for large-scale fluctuation of turbulence energy dissipation,” *Phys. Fluids* **18**, 015103 (2006).

⁷ H. Mouri, A. Hori, and M. Takaoka, “Fluctuations of statistics among subregions of a turbulence velocity field,” *Phys. Fluids* **20**, 035108 (2008).

⁸ H. Mouri, M. Takaoka, A. Hori, and Y. Kawashima, “Probability density function of turbulent velocity fluctuations,” *Phys. Rev. E* **65**, 056304 (2002).

⁹ H. Mouri, M. Takaoka, A. Hori, and Y. Kawashima, “Probability density function of turbulent velocity fluctuations in a rough-wall boundary layer,” *Phys. Rev. E* **68**, 036311 (2003).

¹⁰ K. R. Sreenivasan and B. Dhruva, “Is there scaling in high-Reynolds-number turbulence?,” *Prog. Theor. Phys. Suppl.* **130**, 103 (1998).

¹¹ The alternative interpretation is that such fluctuations correspond to spatial fluctuations of some virtual turbulence. Local values of $u(x)$ and $v(x)$ represent local regions of actual turbulence, and they are continuously connected up to largest scales (see also Appendix of Ref. 6).

¹² The two wires individually respond to all the u , v , and w components. Since the measured u component corresponds to the sum of the responses of the two wires, it is contaminated with the w component. Since the measured v component corresponds to the difference of the responses, it is free from the w component.

¹³ A. N. Kolmogorov, “A refinement of previous hypotheses concerning the local structure of turbulence in a viscous incompressible fluid at high Reynolds number,” *J. Fluid Mech.* **13**, 82 (1962).

¹⁴ E. A. Novikov, “Intermittency and scale similarity in the structure of a turbulent flow,” *J. Appl. Math. Mech.* **35**, 231 (1971).

¹⁵ The velocity derivative $\partial_x v$ was estimated as $[8v(x+\delta x) - 8v(x-\delta x) - v(x+2\delta x) + v(x-2\delta x)]/12\delta x$ with $\delta x = U/f_s$. Even if it is estimated as $[v(x+\delta x) - v(x)]/\delta x$, the results are essentially the same.

¹⁶ J. A. Domaradzki and R. S. Rogallo, “Local energy transfer and nonlocal interactions in homogeneous, isotropic turbulence,” *Phys. Fluids A* **2**, 413 (1990).

¹⁷ K. Ohkitani and S. Kida, “Triad interactions in a forced turbulence,” *Phys. Fluids A* **4**, 794 (1992).

¹⁸ P. D. Mininni, A. Alexakis, and A. Pouquet, “Large-scale flow effects, energy transfer, and self-similarity on turbulence,” *Phys. Rev. E* **74**, 016303 (2006).

¹⁹ W. Feller, *An Introduction to Probability Theory and its Applications*, 2nd ed. (Wiley, New York, 1971), Vol. 2, Chap. 8.4.

²⁰ K. Kajita and T. Gotoh, “Statistics of the energy dissipation rate in turbulence,” in *Statistical Theories and Computational Approaches to Turbulence*, edited by Y. Kaneda and T. Gotoh (Springer, Tokyo, 2003), p. 260.

²¹ The skewness and flatness factors of $\ln v_R^2$ remain close to the Gaussian values. This is because, when the standard deviation is small, a Gaussian distribution is approximated by a lognormal distribution. Although the opposite could be also true, we have ascertained that quantities such as $\delta v_{r,R}^2$ at $R/L_u \lesssim 10^2$ are lognormal rather than Gaussian.

²² L. D. Landau and E. M. Lifshitz, *Statistical Physics*, 3rd ed. (Pergamon, Oxford, 1980), Pt. 1, Chap. 12.

²³ A. N. Kolmogorov, “The local structure of turbulence in incompressible viscous fluid for very large Reynolds numbers,” *Dokl. Akad. Nauk SSSR* **30**, 301 (1941).

²⁴ C. Beck and E. G. D. Cohen, “Superstatistics,” *Physica A* **322**, 267 (2003).

²⁵ V. R. Kuznetsov, A. A. Praskovsky, and V. A. Sabelnikov, “Fine-scale turbulence structure of intermittent shear flows,” *J. Fluid Mech.* **243**, 595 (1992).

²⁶ A. A. Praskovsky, E. B. Gledzer, M. Y. Karyakin, and Y. Zhou, “The sweeping decorrelation hypothesis and energy-inertial scale interaction in high Reynolds number flows,” *J. Fluid Mech.* **248**, 493 (1993).

²⁷ K. R. Sreenivasan and G. Stolovitzky, “Statistical depen-

dence of inertial range properties on large scales in a high-Reynolds-number shear flow," *Phys. Rev. Lett.* **77**, 2218 (1996).

²⁸ S. Kurien and K. R. Sreenivasan, "Anisotropic scaling contributions to high-order structure functions in high-Reynolds-number turbulence," *Phys. Rev. E* **62**, 2206 (2000).

²⁹ R. A. Antonia and P. Burattini, "Approach to the 4/5 law in homogeneous isotropic turbulence," *J. Fluid Mech.* **550**, 175 (2006).